



# Journal of Applied Sciences

ISSN 1812-5654

**science**  
alert

**ANSI***net*  
an open access publisher  
<http://ansinet.com>

## Synthesis and Characterize of Bi<sub>0.6</sub>Sb<sub>1.4</sub>Te<sub>3</sub> Nano-particles from Long Pulsed Laser Ablation

<sup>1</sup>W. Phae-ngam, <sup>1</sup>V. Kosalathip, <sup>1</sup>T. Kumpeerapun, <sup>1</sup>P. Limsuwan and <sup>2</sup>A. Dauscher

<sup>1</sup>Department of Physics, King Mongkut's University of Technology, Thonburi Bangkok 10140, Thailand

<sup>2</sup>Institute Jean Lamour, UMR 7198 CNRS-Nancy Université-Université Paul Verlaine de Metz, Ecole Nationale Supérieure des Mines de Nancy, Parc de Saurupt, CS 4234, 54042 Nancy Cedex, France

**Abstract:** Long pulsed laser ablation was applied to synthesis Bi<sub>0.6</sub>Sb<sub>1.4</sub>Te<sub>3</sub> nano-sized particles of corresponding bulk target in argon environment. Normally, short laser pulses, nanosecond or less, have been used. This work involves with an economical technique involving a Nd:YAG laser working at 1064 nm and millisecond long pulses. System operating parameters including laser frequency (1 Hz), pulse duration variation (1, 3, 5 msec) and target speed at 3000 rpm (2.2 m sec<sup>-1</sup>) were held constant. The particles produced by laser ablation have been characterized by scanning electron microscopy and X-ray diffraction for the morphology and the crystallographic structure of the nano-particles. The experiment shows that the particles were produced in the form of aggregates of primary particle in the nanometer size range between 20 and 120 nm depend on irradiation laser fluence. This technique can prepare mass production of nano-particles in a very short time when compare to femtosecond or nanosecond laser.

**Key words:** Long pulsed laser ablation, nano-particles, thermoelectric, bismuth antimony telluride

### INTRODUCTION

Several techniques for preparation of different nanoparticles such as hydrothermal method for Al doped ZnO (Suliman and Tang, 2007), reduction and microwave heating for Au (Mohamad *et al.*, 2010) while anode support system for Cu<sub>2</sub>O (Abdulkarem *et al.*, 2007) and using of plant to biosynthesis of silver nanoparticles had been reported recently. In this work, a new method of long pulsed laser ablation technique has been employed in the preparation of Bi<sub>0.6</sub>Sb<sub>1.4</sub>Te<sub>3</sub> nanoparticles.

The modern history of laser ablation begins with the discovery of the ruby laser by Maiman in 1960 and the first published account of ablation is the abstract of a talk given by F. Breech and L. Cross at the International Conference on Spectroscopy at the University of Maryland in June 1962 (Miller, 1993). The Pulse Laser Ablation (PLA) is a process for removing material from a solid surface by irradiating it with a laser beam. The PLA can apply to many applications such as laser cleaning of a medieval wooden panel chamber (Wiedemanna *et al.*, 2000), etching of GaN film by UV laser at 266 nm (Zhang *et al.*, 1998), ablation of ZrO<sub>2</sub> and CeO<sub>2</sub> by different laser pulse duration and thin films deposition by Nd:YAG laser at 1064, 532 and 355 nm, an ArF excimer

laser at 248 nm and a Nd:glass laser at 529 nm (Guidoni *et al.*, 2000), annealing treatment of Bi (Pb)-Sr-Ca-O thin film (Jannah *et al.*, 2009) and preparation of conventional thermoelectric nanopowders in water by Nd:YAG laser at 532 nm (Kosalathip *et al.*, 2008).

Generally, PLA use short laser pulses between femtosecond to nanosecond with low speed moving target so they are expensive laser mechanism (Rudolph *et al.*, 1999). The femtosecond laser was used to prepare metal nano-particles. Tsuji *et al.* (2003) presented the silver nano-particles synthesize by femtosecond laser ablation when increased laser wavelength influence particle size increasing. Our study a new technique for synthesis allow nano-particles by long laser pulses in order of microsecond while the target is moving at high speed under argon pressure. By the target is a thermoelectric material of bismuth antimony telluride. Thermoelectric devices are the possible candidates to generate direct electricity from the available thermal radiation as well as other heat sources and have many types of compound on used temperature. Bismuth antimony telluride is a famous thermoelectric material on room-temperature. The efficiency of a thermoelectric material application is determined by the dimensionless figure of merit, defined as:  $ZT = S^2\sigma T/k$ . Where S,  $\sigma$ , k and

T are the Seebeck coefficient, electrical conductivity, thermal conductivity and absolute temperature, respectively. Hostler *et al.* (2008) study the particle-size influential to thermoelectric properties. That work was show the technique of improvident thermoelectric efficiency of bismuth bulk by used low-dimensional structures a pellet composed of bismuth nano-particles. In the aim of this research is to use the alternative low cost to improve morphology, size and crystal structure for thermoelectric material.

**MATERIALS AND METHODS**

The target materials were compound of Bi, Sb and Te in  $\text{Bi}_{10}\text{Sb}_{14}\text{Te}_3$  stoichiometry and were 15 mm in diameter and 3 mm in height which were prepared as described by hot-pressing method (Kumpeerapun *et al.*, 2006). They were cleaned with acetone in an ultrasonic cleaner and mounted on a high speed motor in argon chamber at atmospheric pressure and were radiated at normal incident using convex lens of focal length  $f = 50 \text{ mm}$  at 1064 nm (Fig. 1). The speed of the motor has been fixed at 3000 rpm or  $2.20 \text{ m sec}^{-1}$  (at 15 mm diameter). The pulse duration of the laser beam has been varied from 1 to 10 msec. The output energy is 0.5 J/pulse. The laser used for this work is a pulsed Nd: YAG laser working at 1064 nm. First, a heat effect zone at the surface of the target after interacted by laser pulses when difference pulse durations ranging 1 ms to 5 ms and high moving target speed at  $2.20 \text{ m sec}^{-1}$  was studied. After obtained and characterized the morphology, the particle size and target surface were analyzed by using a Scanning Electron Microscope (SEM). The crystallographic structural of the obtained nanoparticles were determined by X-Ray Diffraction (XRD). In this case, the nano-particles in the form of spherical in chains which flown away from the target were collected at the 20 mm in diameter of cylinder substrate. A thick black layer of nanopowder was obtained for XRD measurements.

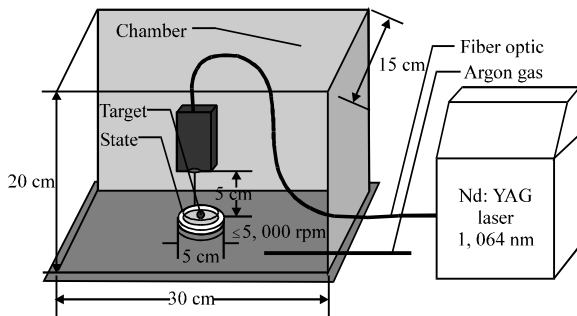


Fig. 1: Diagram of experiment setting

**RESULTS AND DISCUSSION**

**Laser interaction:** Initially, the effects of pulse duration of a laser beam shot on non-moving target and on high speed of 3000 rpm ( $2.20 \text{ m sec}^{-1}$ ) were investigated by varying the pulse durations between 1 to 5 msec. Figure 2 and 3 show the surface of heat-zone for

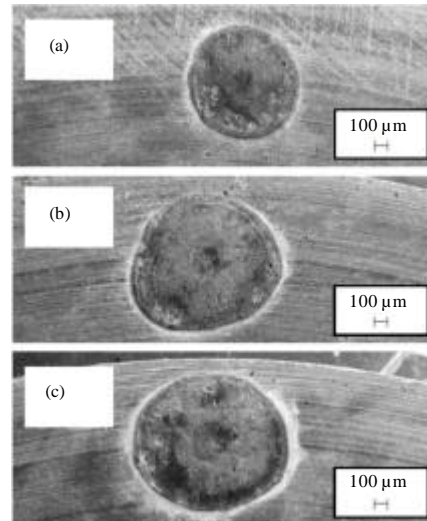


Fig. 2: SEM images of heat-zone surface on non-moving target, (a) 1 msec, (b) 3 msec and (c) 5 msec pulse durations

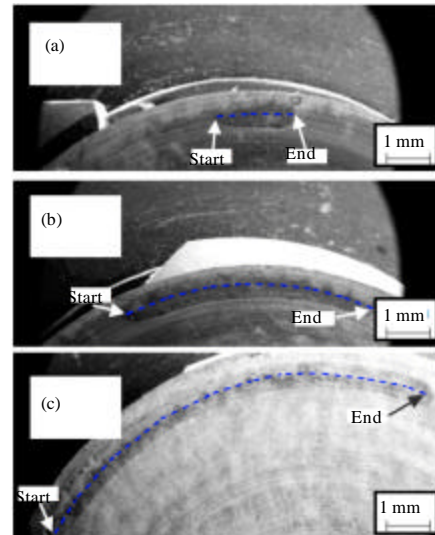


Fig. 3: SEM images of heat-zone surface on moving target at  $2.20 \text{ m sec}^{-1}$ , (a) 1 msec, (b) 3 msec and (c) 5 msec pulse durations

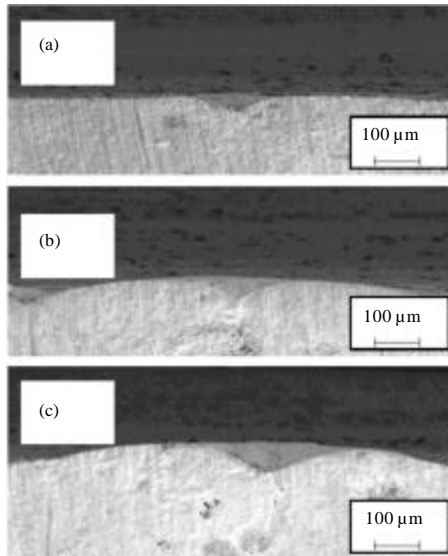


Fig. 4: Cross sectional SEM images of non-moving target, (a) 1 msec, (b) 3 msec and (c) 5 msec pulse durations

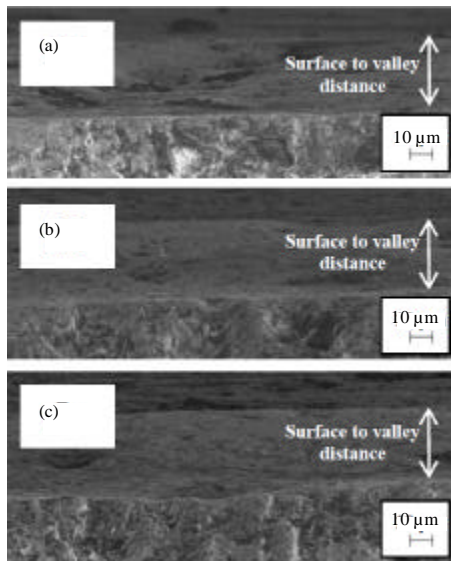


Fig. 5: Cross sectional SEM images of moving target at  $2.20 \text{ m sec}^{-1}$ , (a) 1 msec, (b) 3 msec and (c) 5 msec pulse durations

non-moving and moving targets with the pulse durations were set at 1, 3 and 5 msec, respectively. Figure 2 shows the top view of melting area by single pulse laser interaction on non-moving target. The diameters of melting zone increases from 0.93, 1.16 and 1.30 mm and

laser fluences increases from 7.36, 18.92 and  $24.11 \text{ J cm}^{-2}$  as the pulse durations increase from about 1, 3 and 5 msec, respectively. Figures 4 are cross section of non-moving conditions. The melting depth-hilliness distances increases from 40, 60 and 73  $\mu\text{m}$  as the pulse duration increase from about 1, 3 and 5 ms, respectively. The laser beam interacts to surface, the target is melting and then inflating because of it's cooling down. When the higher energy used, the melting and inflating zones are broad compares to the lower energy. Figure 5 shows cross section of moving conditions, the melting depth distances about 40  $\mu\text{m}$  at every conditions of pulse duration due to the moving target decrease laser fluences.

**Nanoparticles morphological:** Initially, the effects of one shot from the laser beam on the target surface while the target was moving at the high speed of 3000 rpm ( $2.20 \text{ m sec}^{-1}$ ) and non-moving condition when varying the pulse durations between 1 to 5 msec were studied. Figure 2 and 3 show that the heat-zone on surface of non-moving target and cross section by setting pulse duration at 1, 3 and 5 msec, respectively. The SEM image in Fig. 6a-c show the appearance and particle sizes obtained from the difference pulse durations at the same target speed ( $2.20 \text{ m sec}^{-1}$ ). The results shown the particle size distribution obtained from lower fluence is smaller than the higher fluence and the particle size mostly are in range of 10 to 120 nm as in Figure 6d. The average size of outcome nanoparticles 42.24, 48.96 and 55.70 nm are obtain from 1, 3 and 5 msec pulse durations, respectively.

For the morphology, the short colony and amount of nanoparticles was obtained from 1 ms laser pulse duration while longer pulse durations, 3 and 5 ms, give the more amount and longer chain of nanoparticles, the accumulation are rarely occur (Fig. 6a-c).

When the longer pulse duration of the laser beam was applied (Fig. 2-5), the larger area and deeper heat effect zone was created. This shows that more particles and larger particles could be formed from the larger melt volume due to the longer pulse duration of laser beam. The deeper of the heat effect zone near the center could create the larger size of the particles. The smaller size of the particles could come from the melting area which is far away from the center of the melting zone. This means that the thin layer of the melting zone created the formation of the smaller size of nanoparticles while the thick layer of the melting zone created the larger size of nanoparticles Fig. 6d could be used to support this concept. Other than that the longer chain of the groups of nanoparticles were also created due to larger volume of the melting target when the longer pulse duration of laser beam was applied. The pulse duration also effecting the particle size, the

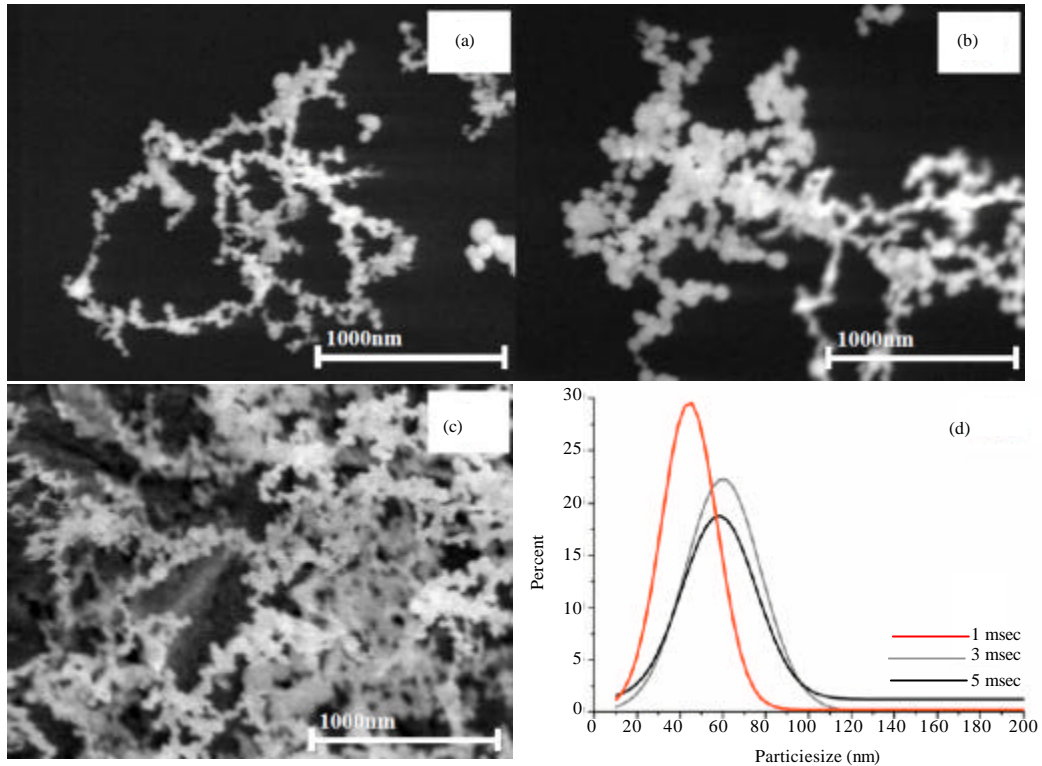


Fig. 6: SEM images of  $\text{Bi}_{0.6}\text{Sb}_{1.4}\text{Te}_3$  nanoparticles were prepared when difference pulse durations at (a) 1 msec, (b) 3 msec and (c) 5 msec and (d) size distribution

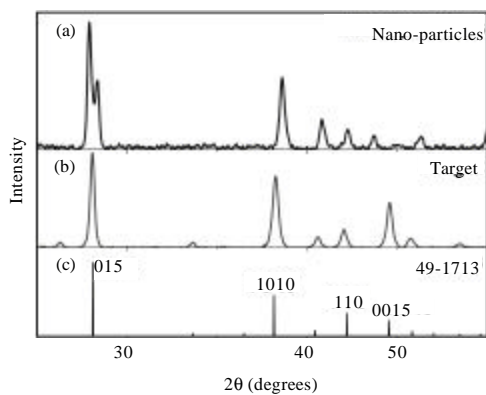


Fig. 7: Crystallographic structure of (a)  $\text{Bi}_{0.6}\text{Sb}_{1.4}\text{Te}_3$  nanoparticles, (b)  $\text{Bi}_{0.6}\text{Sb}_{1.4}\text{Te}_3$  target and (c) JCPDS file number 49-1713

used of shorter pulse duration has been shown the produce smaller particle size as also had been reported in the synthesizing of thermoelectric nanopowders (<35 nm) with pulse duration of 7 ns (Kosalathip *et al.*, 2008).

**Nanoparticles crystal structural:** The crystal structures of target and nanoparticles from 5 ms pulse duration were used to characterize by XRD (Fig. 7). The XRD pattern present the dominate peak at  $2\theta = 28^\circ$ . This peak could neither be attributed to one of simple elements, Bi, Te, or Sb, nor to any known compound indexed in the JCPDS files. The unknown peak also appeared similar to the work of Kosalathip *et al.* (2008) who prepared their nanoparticles in liquid medium. The XRD pattern obtained were correspond to JCPDS 49-1713 of bismuth antimony telluride in rhombohedra structure and showed (0 1 5), (1 0 10), (1 1 0) and (0 0 15) reflection.

## CONCLUSIONS

This work shows a simple and low cost method to synthesize nanoparticles of complex composition, obtained from  $\text{Bi}_{0.6}\text{Sb}_{1.4}\text{Te}_3$  target by long laser pulses in argon atmospheric. This method uses decreasing laser fluence technique and takes a short time preparation and no further treatment necessary. The cost of millisecond pulse laser is much cheaper than the nanosecond pulse laser. There are no needs to use a high cost vacuum

system or liquid medium container. The particle morphology and size were changed by difference pulse duration. The particle preparing process uses long laser pulse cause melting target and spread by rotate speed.

#### ACKNOWLEDGMENTS

The authors are thankful to Human Resource Development in Science Project (Science Achievement Scholarship of Thailand, SAST).

#### REFERENCES

- Abdulkarem, A., E.A. Ammar, Y. Ying and L.J. Lin, 2007. Preparation of Cu<sub>2</sub>O from TiO<sub>2</sub> and CTAB using the anode support system. *J. Applied Sci.*, 7: 4674-4678.
- Guidoni, A.G., C. Flaminia, F. Varsanoa, M. Riccio, R. Teghile, V. Marottab and T.M.D. Palma, 2000. Ablation of transition metal oxides by different laser pulse duration and thin films deposition. *Applied Surf. Sci.*, 154-155: 467-472.
- Hostler, S.R., Y.Q. Qu, M.T. Demko, A.R. Abramson, X. Qiu and C. Burda, 2008. Thermoelectric properties of pressed bismuth nanoparticles. *Superlattices Microstruct.*, 43: 195-207.
- Jannah, A.N., S.A. Halim and H. Abdullah, 2009. Annealing treatment of Bi (Pb)-Sr-Ca-Cu-O Thin Films on MgO by pulsed laser deposition. *J. Applied Sci.*, 9: 2190-2193.
- Kosalathip, V., A. Dauscher, B. Lenoir, S. Migot and T. Kumpeerapun, 2008. Preparation of conventional thermoelectric nanopowders by pulsed laser fracture in water: Application to the fabrication of a pn hetero-junction. *Applied phys. A Mater. Sci. Process.*, 93: 235-240.
- Kumpeerapun, T., H. Scherrer, J. Khedari, J. Hirunlabh and S. Weber *et al.*, 2006. Performance of low-cost thermoelectric modules fabricated from hot pressing and cold pressing material. *Proceedings of the 25th International Thermoelectrics Conference*, Aug. 6-10, Vienna, Austria, pp: 136-140.
- Miller, J.C., 1993. A brief history of laser ablation. *AIP Conf. Proc.*, 288: 619-622.
- Mohamad, M.F., K.S.N. Kamarudin, N.N.F.N.M. Fathilah and M.S. Mohamed, 2010. Effects of PVP concentration on the formation of size and shape of gold (Au) nanoparticles for mercury adsorption. *J. Applied Sci.*, 10: 3374-3378.
- Rudolph, P., J. Bonse, J. Kruger and W. Kautek, 1999. Femtosecond and nanosecond-pulse laser ablation of bariumaluminumborosilicate glass. *Applied phys. A Mater. Sci. Process.*, 69: 763-766.
- Suliman, A.E. and Y. Tang, 2007. Preparation and properties of Zinc oxide doped with aluminum nanostructured thin film. *J. Applied Sci.*, 7: 314-316.
- Tsuji, T., T. Kakita and M. Tsuji, 2003. Preparation of nano-size particles of silver with femtosecond laser ablation in water. *Applied Surf. Sci.*, 206: 314-320.
- Wiedemanna, G., M. Schulzb, J. Hauptmanna, H.G. Kusch, S. Mullera, M. Panznera and H. Wusta, 2000. Laser cleaning applied in the restoration of a medieval wooden panel chamber at Pirna. *J. Cult. Heritage*, 1: 247-258.
- Zhang, J., K. Sugioka, S. Wada, H. Tashiro and K. Midorikawa, 1998. Study on high-speed melting depth etching of GaN film by UV laser ablation. *J. Cryst. Growth*, 189-190: 725-729.